



Rapid assessment of seismic landslide zones

Haiqiang Guo¹  · Lingkan Yao^{1,2,3} · Shaowei Sun¹

Received: 19 March 2015 / Revised: 14 July 2015 / Accepted: 20 July 2015 / Published online: 11 August 2015
© The Author(s) 2015. This article is published with open access at Springerlink.com

Abstract In the feasibility stage of the transport route selection, large-scale geological investigations are advised before the route is determined. Therefore, rapid assessment of seismic landslide zones can be completed by the second development of the ArcGIS program. A large amount of geological information can be obtained by this method which is based on existing remote sensing image data. The integrated data can then be used to guide route location selection. This method assesses the angle between the main axis of the slope and the axis of the route and produces a zoning map that identifies slopes that threaten the route by combining with other characteristics including the climate in the study area, and the lithology and seismic structure of the near-field region. A hazard-zone map showing the degree of earthquake-induced landslide can be quickly generated by the comprehensive index method. The seismic landslide zone map was verified by comparison with the findings of a geological engineering survey conducted in the study area.

Keywords Earthquake · Collapse · Landslide · Hazard zonation · Location design

1 Introduction

Many earthquakes have occurred in China in the 21st century. In the last 5 years, two high-magnitude earthquakes occurred in Sichuan Province (the Ms 8.0 Wenchuan earthquake and the Ms 7.0 Lushan earthquake) [1–3]. Both earthquakes induced a large number of landslides that caused serious damage to roads. Statistical data show that landslide disasters triggered by the Ms 8.0 Wenchuan earthquake damaged nearly 28,000 km of highway (including 21 expressways, 15 national and provincial highways, and 2,795 rural highways) and caused damage to railways (including the Chengguan Railway, Guangyue Railway, Detian Railway, and the Mianyang–Guangyuan segment of the Baocheng Railway). The damaged roads not only caused huge losses of life and property, but also blocked traffic and seriously delayed the rescue operations. Maintaining smooth traffic flow was very challenging [4].

Engineers and transport experts should pay close attention to regional geology when selecting the routes for roads running through rugged mountainous areas based on practice [5]. For a full understanding of the geological disasters and geo-hazards in the route region, detailed geological exploration data must be obtained. However, during the feasibility study stage of route selection, the route schemes are yet to be determined; therefore, generally, no large-scale geological investigation is performed. Hence, it is important to obtain as much geological hazard information as possible in the route area to guide the route planners and engineers by using existing satellite remote sensing data.

Landslides cause serious damage in mountainous regions. Currently, analysis methods of regional slope stability under seismic action include the pseudo-static method and the Newmark slider analysis method. To

✉ Haiqiang Guo
1489535@qq.com

¹ School of Civil Engineering, Southwest Jiaotong University, Chengdu 610031, China

² MOE Key Laboratory of High-speed Railway Engineering, Chengdu 610031, China

³ Road and Railway Engineering Research Institute, Sichuan Key Laboratory of Aseismic Engineering and Technology, Chengdu 610031, China

estimate slope stability, the minimum coefficient of slope stability under seismic action was obtained by Leshchinsky [6], Ling [7], and Biondi [8], and by other methods based on the pseudo-static method. However, there are obvious deficiencies in the pseudo-static method. First, the seismic inertia force is neither invariable nor unidirectional, with rapid fluctuations in both magnitude and direction. Second, a slope coefficient of stability less than 1 will not necessarily lead to an overall slope instability, but may only create a permanent slope displacement. Newmark [9] calculated the deformation of a dam caused by an earthquake using the slider model. Subsequently, the Newmark method was combined with GIS by Jibson [10–12], Miles [13], and Rodríguez-Peces [14]. Using GIS technology, they divided the study area into grids of different sizes and each grid was seen as an independent slope. Then the seismic landslide hazard classification for the study area was performed according to the displacement size. Although this method has great advantages for prediction of regional landslide triggered by earthquakes, the stability of slopes is also strongly affected by the structural features and characteristics of the slope, the rock and soil composition, and the general slope of the terrain. Thus, taking these factors into consideration during landslide hazard assessment can greatly improve the accuracy of the predictions.

To improve the estimation accuracy, a method for rapid assessment of seismic landslide hazards was developed. This method uses GIS technology, and divides the slope units according to the geological and hydrogeological conditions. A hazard-zone map for landslides triggered by regional seismic activity can be generated rapidly based on a comprehensive index method. This method can be used to obtain guidelines for initial route selection in high seismic regions and for reconstruction projects along existing routes. This can significantly reduce the work required during the feasibility stage of route selection, and narrow the scope of the geological exploration required for project planning. Correct prevention and mitigation measures can be proposed, project safety improved, and losses caused by design changes reduced.

2 Principle and method of seismic landslide hazard zoning

The principle of the rapid assessment of seismic landslide hazard zones is based on satellite remote sensing data. Combining GIS spatial analysis techniques and statistical methods for seismic landslide analysis, the slope units are determined along pre-built routes and existing reconstruction routes. Then the statistics, identification, and analysis are performed on the slope units. Finally, the seismic

landslide hazard zoning map can be generated. The block diagram of the identification method is shown in Fig. 1.

2.1 Determining the units of the regional slopes

2.1.1 Division of slope units

At present, the slope units are divided mainly into two types: regular grid units and complex slope units. The regular grid units can be easily processed, using a relatively simple calculation method and algorithm. However, this evenly distributed grid unit is not related to the actual failure unit and physical mechanism. It is completely unrelated to the geology, topography, and hydrology. The slope unit is defined as an area with features that are distinct from those of the adjacent regions. The formation of the terrain reflects the long-term effects of the geological conditions and hydrogeological conditions [15–17]. The schematic diagram of the slope (Fig. 2) shows the ridge line and the valley line of the digital topographic map, found through the hydrologic analysis functions of ArcGIS. The catchment area was divided into slope A and slope B defined by the valley lines and ridge line.

The size selection of the slope units depends on the average size of the historic landslide in the study area. For objects with similar topography, geology, and hydrological conditions in the same area, we assume a similar the scale of the past and future landslide failure slopes. When dividing the slope units, the threshold value of the catchment area determines the size of the slope unit. In practice, multiple threshold values are needed and trial calculations are performed to determine the appropriate threshold level.

2.1.2 Hydrological analysis

The hydrological characteristics of the study area are related to the topography of the region. During the rainy

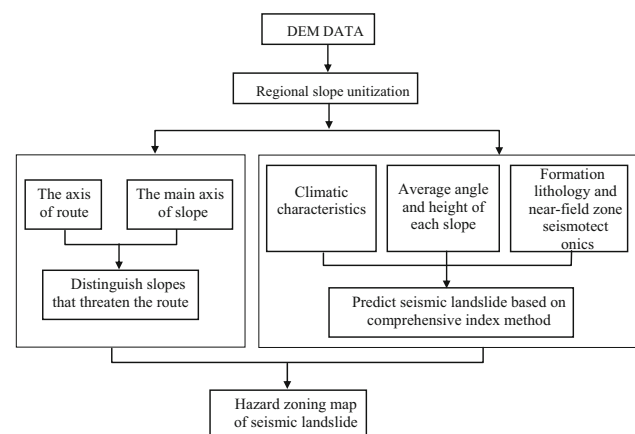


Fig. 1 Block diagram of assessment of seismic landslide hazard zones

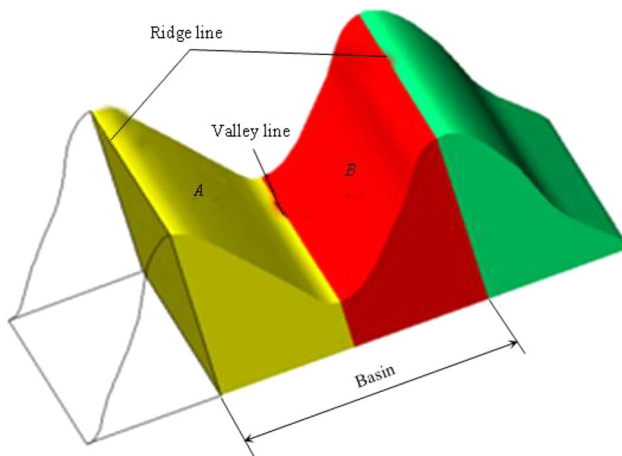


Fig. 2 Schematic diagram of the slope used in our method

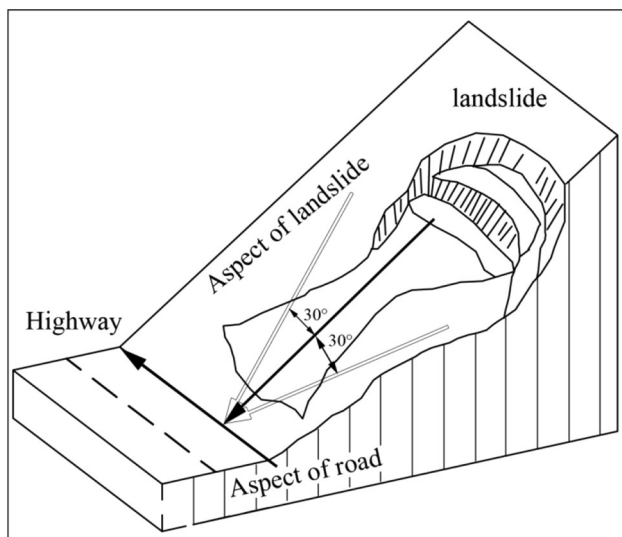


Fig. 3 Illustration of slope angles affecting landslide risk

season in the mountains, some water infiltrates into the ground, and the remaining flows from higher to lower elevation under the force of gravity. Hydrological analysis of the area was carried out using the hydrologic analysis tools of ArcGIS. The hydrological analysis module was used to extract the depression-free digital elevation model (DEM), flow direction, flow collection, channel network generation date, and basin analysis from the DEM. Then the ridge line was obtained. The valley line was extracted by changing the original valley in the model to a ridge. The same method was used to extract the depression-free DEM, flow direction, flow collection, channel network generation, and basin analysis from the inverted DEM and obtain the valley line. When transforming the raster data into polygons, some incorrect polygon slope units may appear: very small polygon slope units and inconsistent

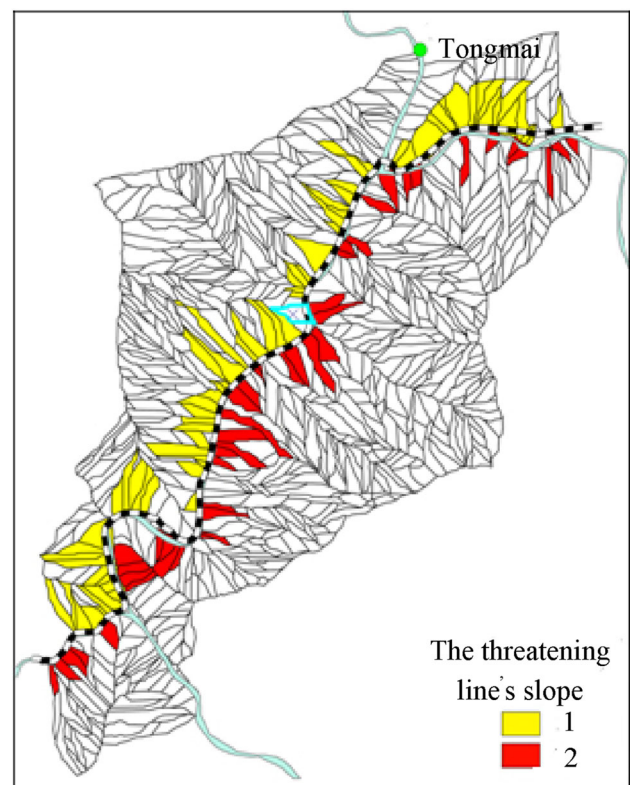


Fig. 4 Zoning map of the slopes threatening the route

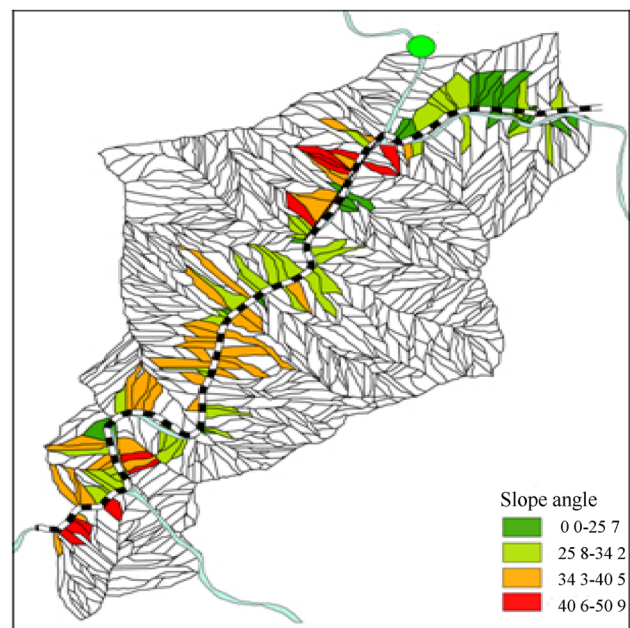


Fig. 5 The average angle of the slopes

polygon slope units. These incorrect polygon slope units can be eliminated by using the 'dissolve' function and the 'integrate' function in GIS. If the result of the division of

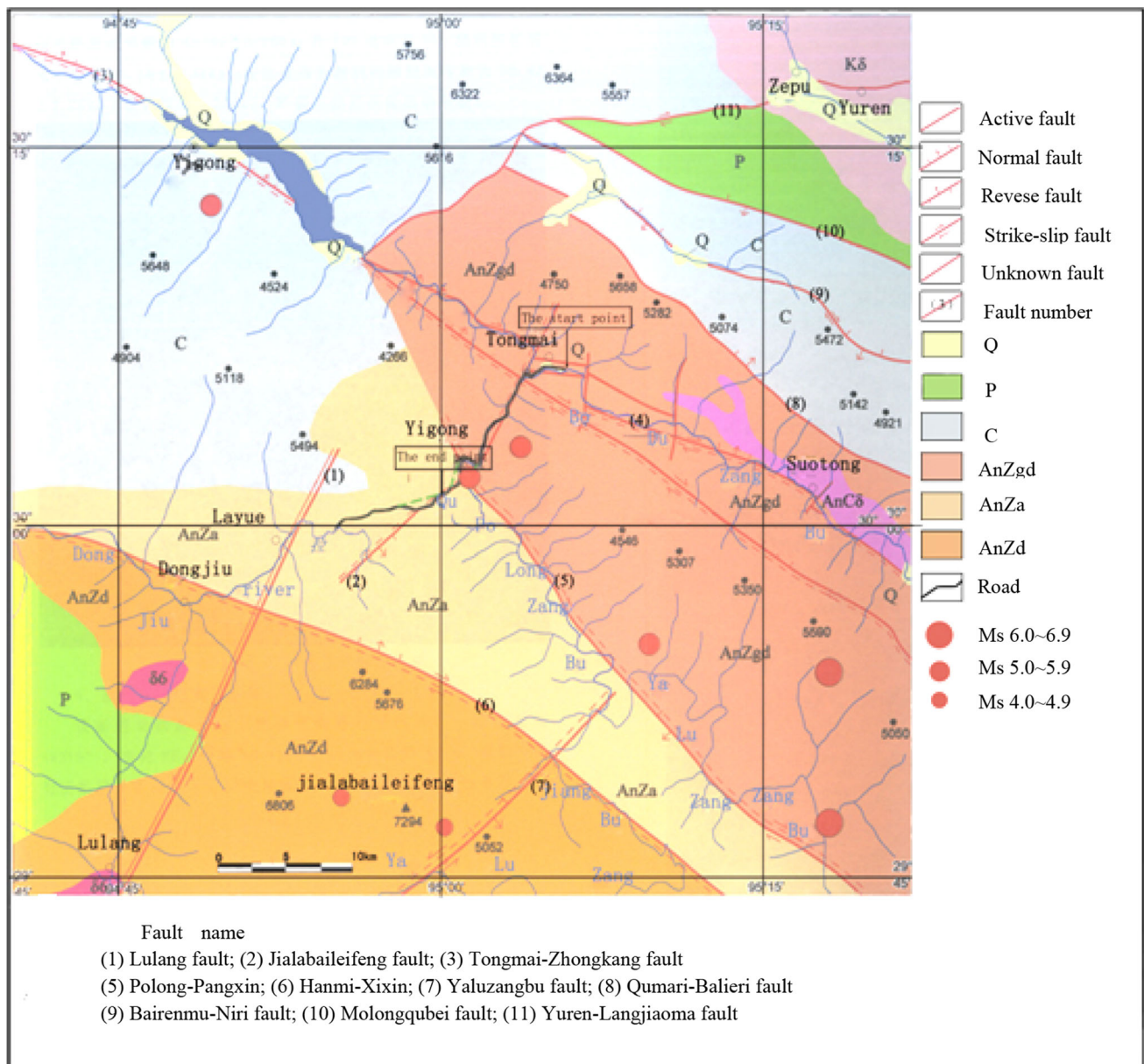


Fig. 6 Seismotectonic map of the region surrounding the Tongmai-105 Road section

the polygon slope units is still unsatisfactory, it can be adjusted by artificial modification.

2.2 Identifying slopes that threaten transport routes

The safety of railway and highway routes in the study area is at high risk from landslides, particularly if the axis of the landslide and the axis of the route intersect at a large angle. A landslide can cause serious damage and injuries when this angle ranges from 60° to 120° (an angle between the slope and the route alignment of -30° to $+30^\circ$), as shown in Fig. 3.

2.3 Prediction of seismic landslide risk based on the comprehensive index method

Based on the obtained map of unstable slope zones in the study area, the comprehensive index method [18] is used to predict seismic landslides that threaten the transport route. This method uses existing earthquake data in China. The variables are the lithology and formation structure, slope height, slope angle, and earthquake and rainfall parameters. The method was verified for seismic landslide prediction in western China. The stability of a slope can be expressed as

$$H = (S_i \times S_a \times S_h) \times (T_s + T_p), \quad (1)$$

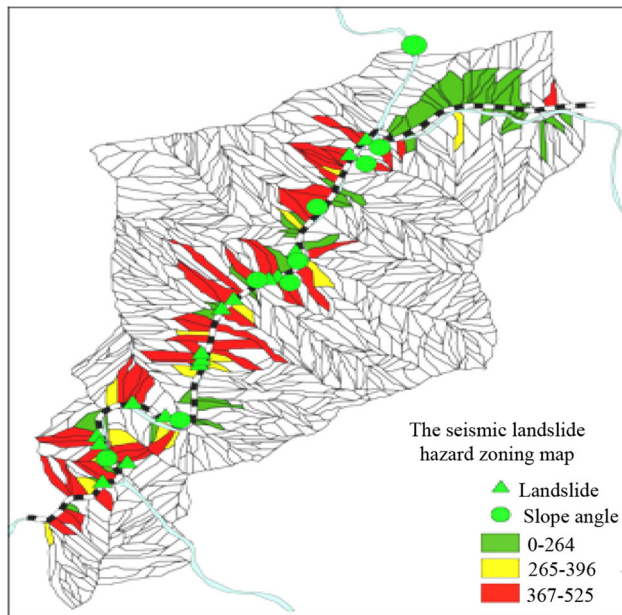


Fig. 7 Seismic landslide hazard-zone map

where S_h is the influence coefficient of slope height, S_l is the condition coefficient of the lithology, S_a is the influence coefficient of the slope angle, T_s is the strength coefficient of the earthquake, T_p is the strength coefficient of the rainfall, and H is the stability of the slope. If $H < 264$, the slope is stable; if $H > 396$, the slope is unstable. When H is between 264 and 396, the stability of the slope is unknown.

Equation (1) indicates that earthquake-induced landslides are caused by a combination of external factors (earthquakes, rainfall) and internal factors (slope height, lithology, and slope angle). Finally, a comprehensive index value that determines the stability of the slopes in the study area is calculated and the critical value for an earthquake-triggered landslide is determined.

3 Case analysis

The 20-km segment of the Tongmai-105 Daoban was selected as our study area, starting east of the Tongmai bridge and ending in the gang's former site. This is an important part of the Sichuan–Tibet highway, and it is an existing route reconstruction project. The section of the road is located in the deep-cutting gorge area of South-eastern Tibet. The region experiences a high level of earthquake activity, the neotectonic movement is strong, and the geological structure is complex. The rock is fragmented, loose, and unstable and rainfall is abundant. A maritime glacier spans a wide area, and the river and water systems are continuously evolving, with strongly down-cutting valleys and gullies. The road section is highly prone

to geological disasters. It is an ideal study area of earthquake-induced landslides. The image data for this region were provided by the Resources Satellite Three and GF-1 satellite. The image accuracy is 1:25,000.

3.1 Division of slopes threatening the route in the study area

A total of 804 slopes were identified in the study area by using the hydrological analysis method. The average aspect of all the grids was calculated for each slope. The angle between the main axis of the slope and the route was evaluated. Any slope that threatens the routes by the second development of the ArcGIS program was identified. Finally, we generated the map of the slope zones that threaten the road, as shown in Fig. 3. The yellow (1) and red zones (2) in Fig. 4 denote the slopes that have a high risk of forming landslides along the route on the east and west sides of the river, respectively, while the white slopes represent slopes that pose little or no threat to the route.

3.2 Assessment of seismic landslide risk in study area

3.2.1 Climatic characteristics of the study area

The climate of the study area is mild and humid. The annual mean temperature is between 8 and 13 °C and the annual precipitation is between 1,000 and 1,400 mm. The rainy season lasts from April to October and the dry season is from November to March. The precipitation during the rainy season accounts for 85.5 % of the total annual precipitation. The rainy seasons are longer than the dry seasons and most of them are moderate. Heavy rain is infrequent and rainstorms do not exceed a daily precipitation of 50.0 mm.

3.2.2 The average angle and height of each slope

The average angle (Fig. 5) and the relative height of each slope unit were calculated in the second development of ArcGIS5.

3.2.3 Lithology and near-field seismotectonics of the study area

According to geological data provided by department of transportation of Tibet, the bottom of the landslide is covered by loose accumulation masses of Quaternary Holocene (colluvium layer (Q_4^{c+dl}), a landslide accumulation layer of Quaternary Holocene (Q_4^{del}), alluvial layer of

Table 1 Landslide along the renovation and reconstruction project in the Tongmai 105 Road segment

Number	Mileage stake number	Length [m]	Quantity [10^4m^3]	Landslide type	Scale	Forming factor	Formation period	Stability
H1	K4092 + 180 – 240	60	0.9	Debris landslide	Small	Rock piles, rain, earthquake, etc.	New landslide	Unstable
H2	K4092 + 505 – 550	45	0.6	Debris landslide	Middle	Rain, earthquake, etc.	New landslide	Unstable
H3	K4095 + 270 – 400	130	7	Debris landslide	Middle	Lateral erosion of Yigongzangbu glacier mudslide in 2000	New landslide	Basically stable
H4	K4096 + 580 – 637	57	1	Debris landslide	Middle	Lateral erosion of river, rain, earthquake, etc.	New landslide	Unstable
H5	K4096 + 660 – 810	150	28	Debris landslide	Large	Lateral erosion of river, rain, earthquake, etc.	Old landslide	Basically stable
H6	K4097 + 200 ± 413	213	22.6	Debris landslide	Large	Lateral erosion of Yigongzangbu glacier mudslide in 2000	New landslide	Basically stable
H7	K4097 + 597	73	1.6	Debris landslide	Middle	Lateral erosion of Yigongzangbu glacier mudslide in 2000	New landslide	Basically stable
H8	K4098 + 260	120	9.2	Debris landslide	Middle	Lateral erosion of Yigongzangbu glacier mudslide in 2000	New landslide	Basically stable
H9	K4098 + 390 ± 451	61	3.7	Debris landslide	Middle	Lateral erosion of Yigongzangbu glacier mudslide in 2000	New landslide	Unstable
H10	K4098 + 451 ± 646	195	10.5	Debris	Large	Lateral erosion of Yigongzangbu glacier mudslide in 2000	New landslide	Unstable
H11	K4101 + 450	–	7.98	Debris landslide	Middle	Lateral erosion of Yigongzangbu glacier mudslide in 2000	New landslide	Unstable
H12	K4101 + 890 – K4102 + 026	136	30	Debris landslide	Large	Rain, earthquake, human engineering work, etc.	Old landslide	Basically stable

Quaternary upper Pleistocene ($Q_3^{\text{al+pl}}$), debris flow accumulation layer of Quaternary Holocene (Q_4^{sef}), and alluvial layer of Quaternary Holocene ($Q_4^{2\text{al+pl}}$). The underlying bedrock consists mainly of the Presinian Gandise rock group (AnZgd) and Presinian Barwa rock group, and the Ani bridge schist group (AnZa), as shown in Fig. 6.

In the study area, seismic waves with $M_s \geq 4.7$ were recorded 115 times, seismic waves with $4.7 \leq M_s \leq 4.9$ 26 times, seismic waves with $5.0 \leq M_s \leq 5.9$ 70 times, seismic of Quaternary Holocene waves with $6.0 \leq M_s \leq 6.9$ 16 times, seismic waves with $7.0 \leq M_s \leq 7.9$ twice, and seismic waves with $M_s \geq 8.0$ once. The earliest recorded earthquake is the Langxianzari 4.75 earthquake in 1331 AD. The largest earthquake (M_s 8.6) occurred at Motuo, Tibet in 1950 [19, 20]. The level of seismic activity in this area is high. The earthquakes are very unevenly distributed spatially; most of the major earthquakes are located in the fault zone. There is a possibility of an earthquake of magnitude ~ 7.0 occurring in the vicinity of the Motou 8.6 earthquake

in the next hundred years but the possibility of an earthquake with a magnitude $M_s 7.5$ is small. There are many records of historical earthquakes that occurred in the area surrounding the study site, some of them of small magnitude; this has affected the geology of the region. Modern earthquakes are more frequent, smaller in magnitude, and have a weaker impact on the region. The earthquake with the highest intensity in the study area was the 8.6 Motuo 8.6 earthquake in 1950; the smallest distance to the field region was only 125.4 km. The near-field seismotectonic region is shown in Fig. 6.

3.2.4 Estimation of earthquake-triggered landslides

We used the method of Ding et al. [18] to produce the hazard-zone map of seismic landslides in the study area (Fig. 7). A total of 126 slopes were found to be a threat to the route. Of these, 58 slopes were predicted unstable, 17

Table 2 Collapses along the renovation and reconstruction project in the Tongmai-105 Road segment

Number	Mileage stake number	Lithological composition of slope	Forming condition	Damage degree
B1	K4093 + 846 – K4094 + 308	Granitic gneiss	Steep slope, evolving joint, fragmented rock	The upper part of the slope is still steep, and can easily collapse
B2	K4095 + 826 – K4096 + 226	Granitic gneiss, thick layer clipping thin layers	Steep slope, joint and fault evolving, fragmented rock	Locally known as the Small Tiger Mouth, large stone dents are common, causing damage to cars and pedestrians
B3	K4096 + 677 – K4096 + 765	Granitic gneiss, thin layers	Steep slope, joint and unloading fissure evolving, fragmented rock	Damage often caused by rainy storm erosion and earthquakes
B4	DK4100 + 110 – DK4100 + 260	Granitic gneiss, two-mica quartz schist, thin layers	Joint and unloading fissure evolving, fragmented rock	Minor effect on the safety of the abutment of Palong Bridge #1
B5	DK4103 + 550 – DK4104 + 230	Two-mica quartz schist, thin layer clipping thick layer shape	Joint and unloading fissure evolving, fragmented rock	This section consists of the collapse group, the upper part of the distribution area is steep, the slope angle is 70–90°, rock collapse is still possible
B6	K4091 + 340 – K4093 + 600 the opposite bank	Granitic gneiss	Steep slope, evolving joint, fragmented rock	General hazard
B7	K4095 + 820 – K4098 + 310 the opposite bank	Granitic gneiss	Steep slope, evolving joint, fragmented rock	General hazard

slopes were possibly unstable, and 51 slopes were estimated as stable.

4 Verification of earthquake-induced landslide hazard zones

The most accurate way to assess landslides and land collapse in the study area is to perform a detailed geological field survey. To verify the accuracy of our seismic landslide hazard zonation map, we compared it with the geological survey reports produced for the renovation reconstruction project in this segment of the route (geological exploration report on this segment provided by the Communications Department of Tibet). The geological survey found 12 landslides posing a great threat to the route along the existing route of the reconstruction project in the Tongmai-105 Road segment. The scale and causes of the landslides are shown in Table 1. There were 7 collapse sites along the project route; their main characteristics are shown in Table 2. In addition, 4 larger landslides were found along the route reconstruction project scheme A. The 23 collapses and landslides mentioned above were marked on the route and compared with our hazard estimation map, as shown in Fig. 7.

Figure 7 shows that of the 23 collapse and landslide sites identified in the geological exploration report, 19 were

identified in our assessment as threats to the route. Only 2 landslide sites (H3, AH1) and 2 collapse sites (B2, B4) were not included in our hazard-zone map as threats to the route. In those sites, the angle between the slope and the route setting is outside the 60–120° range (Sect. 2.2 above). Therefore, they pose a low threat to the route and were excluded from our hazard prediction. Of the remaining 19 collapses and landslide sites, only one landslide (H7) was evaluated incorrectly in our method. The other 18 sites were judged to be unstable in an earthquake, in agreement with the geological survey findings. It should be noted that although not all the collapse and landslide sites identified in the survey were triggered by earthquakes, they are in a dangerous state under static forces. Therefore, these 23 landslides are considered unstable in the event of an earthquake.

Thus, the rapid assessment of seismic landslide hazard zones is a valuable tool for transport route planners and engineers. Its estimation accuracy will be further improved with higher-precision remote sensing image data.

5 Conclusions

Using satellite remote sensing technology, the landslide hazard in rugged mountainous region with active tectonic movement can be well predicted for the determination of

new routes and the reconstruction of existing routes. The seismic-triggered landslide hazard estimation method presented here is especially useful for route location in rugged and dangerous mountain region.

1. A great threat to the safe operation of the route exits if the main axis of the landslide and the route aspect intersect at a large angle. According to the field survey of the study area, the most serious damage occurs when the angle between the main axis of the slope and the axis of route is between 60° and 120° . A map of the slopes that pose a threat to the route can be obtained by identifying the high-risk slopes based on the second development of ArcGIS. By using the method of Ding et al. [18], combined with map of the slopes that threaten route, a hazard-zone map of seismic landslides is obtained. The results were verified by comparing with the results of a geological survey report, confirming its high accuracy.
2. To conduct a feasibility study for railway or highway routes, the presented method can quickly generate a seismic landslide hazard-zone map as a guideline for preliminary route selection. A safety corridor can be rapidly selected and workers in the field can clear the selected route. A comprehensive geological survey can then be carried out along the route and more detailed surveys are performed if high-risk sites are identified. Thus, this method can considerably reduce the project costs as well as save time. Moreover, it will contribute to the safety of the operation by preventing landslide and collapse accidents, and losses due to design changes will be significantly reduced.

Open Access This article is distributed under the terms of the Creative Commons Attribution 4.0 International License (<http://creativecommons.org/licenses/by/4.0/>), which permits unrestricted use, distribution, and reproduction in any medium, provided you give appropriate credit to the original author(s) and the source, provide a link to the Creative Commons license, and indicate if changes were made.

References

1. Qiu YL, Yao LK, Zhu Y, Wei YX (2014) Disaster reduction technique of railway selection in high earthquake intensity mountainous regions. *J Southwest Jiaotong Univ* 49(6):972–980 (in Chinese)

2. Chen YT, Yang ZX, Zhang Y et al (2013) From 2008 Wenchuan earthquake to 2013 Lushan earthquake (in Chinese). *Scientia Sinica Terrae* 43:1064–1072 (in Chinese)
3. Xu XW, Chen GH, Yu GH et al (2013) Seismogenic structure of Lushan earthquake and its relationship with Wenchuan earthquake. *Earth Sci Front* 20(3):11–20 (in Chinese)
4. Yao LK, Chen Q (2009) New research subjects on earthquake resistant techniques of line engineering extracted from 5.12 Wenchuan Earthquake. *J Sichuan Univ* 41(3):43–50 (in Chinese)
5. Zhu Y (2009) Innovation and practice on railway location concept. *J Railw Eng Soc* 129(6):1–5 (in Chinese)
6. Leshchinsky D, San KC (1994) Pseudo-static stability of slopes: design. *J Geotech Eng* 120(9):1514–1532
7. Ling HI, Cheng AHD (1997) Rock sliding induced by seismic force. *Int J Rock Mech Min Sci* 34(6):1021–1029
8. Biondi G, Cascone E, Maugeri M (2002) Flow and deformation failure of sandy slopes. *Soil Dyn Earthquake Eng* 22(9):1103–1114
9. Newmark NM (1965) Effects of earthquakes on dams and embankments. *Geotechnique* 15(2):139–160
10. Jibson RW (2007) Regression models for estimating coseismic landslide displacement. *Eng Geol* 91(2):209–218
11. Jibson RW (2011) Methods for assessing the stability of slopes during earthquakes—a retrospective. *Eng Geol* 122(1):43–50
12. Jibson RW, Harp EL, Michael JA (2000) A method for producing digital probabilistic seismic landslide hazard maps. *Eng Geol* 58(3):271–289
13. Miles SB, Ho CL (1999) Rigorous landslide hazard zonation using Newmark's method and stochastic ground motion simulation. *Soil Dyn Earthq Eng* 18(4):305–323
14. Rodríguez-Peces MJ, García-Mayordomo J, Azañón JM et al (2014) GIS application for regional assessment of seismically induced slope failures in the Sierra Nevada Range, South Spain, along the Padul Fault. *Environ Earth Sci* 72(7):2423–2435
15. Xie MW, Cai MF, Esaki T (2006) GIS-based three-dimensional slope stability limit equilibrium method and application. *Rock Soil Mech* 27(1):117–122 (in Chinese)
16. Xie MW, Esaki T, Zhou GY (2003) GIS method for slope-unit-based 3D landslide hazard evaluation. *Chin J Rock Mech Eng* 22(6):969–976
17. Xie MW, Esaki T, Zhou G, Mitani Y (2003) GIS-based 3D critical slope stability analysis and landslide hazard assessment. *J Geotech Geoenviron Eng* 129:1109–1118
18. Ding YH, Wang YQ, Sun JZ et al (2000) Research on the method for prediction of earthquake induced landslides and its application to engineering projects. *J Eng Geol* 08(04):475–480 (in Chinese)
19. Liu YH (1985) Study of the macroscopic seismic hazard and the intensity features of the motuo earthquake, tibet. *J Seismol Res* 8(5):477–483 (in Chinese)
20. Shao CR, You HC, Cao ZQ (2008) Tectonic characteristics and seismic activities of Yaluzangbu Grand Canyon, Tibet. China. *Technol Earthq Disaster Prev* 38(4):398–412 (in Chinese)